

Total Hadronic Cross Sections and $\pi^\mp\pi^+$ Scattering

Francis Halzen^{a*}, Keiji Igi^{b†}, Muneyuki Ishida^{c‡}, C. S. Kim^{d§}

^a Department of Physics, University of Wisconsin, Madison, WI 53705, USA

^b Mathematical Physics Laboratory, RIKEN Nishina Ctr., Wako, Saitama 351-0198, Japan

^c Department of Physics, Meisei University, Hino, Tokyo 191-8506, Japan

^d Department of Physics & IPAP, Yonsei University, Seoul 120-749, South Korea

Abstract

Recent measurements of the inelastic proton-proton cross section at the LHC and at cosmic ray energies by the Auger experiment have confirmed fits to lower energy data based on the simple idea that the proton is asymptotically a black disk of gluons. In this context, we show that data on $\bar{p}(p)p$, $\pi^\mp p$, and $K^\mp p$ forward scattering support the related expectation that the asymptotic behavior of all cross sections is flavor independent. By using the most recent measurements from ATLAS, CMS and Auger, we predict $\sigma_{\text{tot}}^{pp}(\sqrt{s} = 14 \text{ TeV}) = 108.1 \pm 1.4 \text{ mb}$, as well as refine the total cross sections $\sigma_{\text{tot}}^{pp}(\sqrt{s} = 7 \text{ TeV}) = 96.1 \pm 1.1 \text{ mb}$ and $\sigma_{\text{tot}}^{pp}(\sqrt{s} = 57 \text{ TeV}) = 135.7 \pm 2.2 \text{ mb}$. We use our results also to predict the total $\pi^\mp\pi^+$ cross sections as a function of \sqrt{s} .

*francis.halzen@icecube.wisc.edu

†igi@phys.s.u-tokyo.ac.jp

‡mishida@wisc.edu

§cskim@yonsei.ac.kr

1 Introduction

Recent high energy measurements of the inelastic proton-proton cross section, made possible by the Large Hadron Collider (LHC) and a new generation of cosmic ray experiments, have convincingly confirmed [1] indications [2, 3, 4, 5] in lower energy data that the total cross section σ_{tot} behaves asymptotically as the squared log of the center-of-mass energy \sqrt{s} , consistent with the energy dependence of the Froissart unitarity bound [6]. The COMPETE Collaboration has further proposed that this asymptotic behavior $\sigma_{\text{tot}} \simeq B \log^2(s/s_0)$ applies to all hadron total cross sections, with a universal value of B [3, 7]. The universality of B was theoretically anticipated in Refs. [8, 9] and recently inferred from a color glass condensate [10, 11] of QCD. The interpretation of the Froissart bound was presented [12] in the context of QCD, and the value of the universal constant $B \simeq 0.3$ mb further suggests that the unitarity bound is saturated. However, there is still no rigorous proof based only on QCD, although the simplest interpretation of the present data is that, asymptotically, particles of all flavors evolve in a black disk of gluons.

In order to empirically test this universality, the $\bar{p}(p)p, \pi^\mp p$, and $K^\mp p$ forward scattering amplitudes are analyzed, and the values of B , denoted respectively as $B_{pp}, B_{\pi p}$, and B_{Kp} , were estimated independently [13]. The analysis was refined [14] for B_{Kp} . The resulting values are consistent with the universality, $B_{pp} \simeq B_{\pi p} \simeq B_{Kp}$, and thus, the universality of B is suggested. In this letter we first update the analysis of the $\bar{p}(p)p, \pi^\mp p$, and $K^\mp p$ data by including newly measured LHC results as well as very high energy measurements based on cosmic ray data. Subsequently, assuming the universality of B , we calculate the $\pi^\mp\pi^+$ total cross section $\sigma_{\text{tot}}^{\pi^\mp\pi^+}(s)$ at all energies.

Although challenging, the data on $\pi^\mp\pi^+$ collisions could be extended to higher energies exploiting high intensity proton beam accelerator beams planned worldwide, such as Project X [15] of FNAL and J-PARC in Japan [16]. At a later stage these may develop into muon colliders. As an example, Project X, a high intensity proton source proposed at Fermilab, would deliver proton beams at energies ranging from 2.5 to 120 GeV [15] and secondary pion beams with $E(\pi) \approx 2 - 15$ GeV. A muon collider with Project-X-intensity pion beams would represent a $\pi^+\pi^-$ collider with $\sqrt{s} = 1$ TeV and a luminosity of $10^{22} \text{cm}^{-2}/\text{sec}$ [17], not quite sufficient, even for measuring the large cross sections discussed here. Some manipulation of the secondary beams would be required. On the other hand, direct measurements of $\sigma_{\text{tot}}^{\pi\pi}$ in wide range of pion beam energy would be made possible. In the absence of such measurements we will extend our calculations of $\sigma_{\text{tot}}^{\pi^\mp\pi^+}(s)$ into the intermediate energy region using Regge theory. This will allow us to compare our predictions with indirect information [18, 19] extracted from processes such

as $\pi^- p \rightarrow \pi^- \pi^+ n$, $\pi^- \pi^- \Delta^{++}$, assuming one-pion-exchange dominance.

2 Update of the fits to σ_{total}

2.1 Analysis of Forward $\bar{p}(p)p, \pi^\mp p, K^\mp p$ Amplitudes

The energy (momentum) of the beam in the laboratory system is denoted by $\nu(k)$. It is related to the center of mass energy \sqrt{s} by

$$s = 2M\nu + M^2 + m^2, \quad \nu = \sqrt{k^2 + m^2} \quad , \quad (1)$$

where $m = M, \mu, m_K$ for $pp, \pi p, Kp$ scattering, and M , μ , and m_K are proton, pion and kaon masses; respectively. $s \simeq 2M\nu$ in high-energies.

The crossing-even forward scattering amplitude, $F_{ab}^{(+)}(\nu)$, is given by the sum of Pomeron and Reggeon (including P' trajectory) exchange terms, while the crossing-odd $F_{ab}^{(-)}(\nu)$ is given by a single contribution from Reggeon (corresponding to vector-meson trajectories) exchange contributions. Here the subscripts ab and $\bar{a}\bar{b}$ represent $ab = pp, \pi^+ p, K^+ p$ and $\bar{a}\bar{b} = \bar{p}p, \pi^- p, K^- p$, respectively. We consider the exchange degenerate $f_2(1270)-$, $a_2(1320)$ -trajectories for the crossing-even Reggeon (tensor-meson) term and the ρ -, ω -trajectories for the vector-meson term. Their imaginary parts are given explicitly by

$$\text{Im } F_{ab}^{(+)}(\nu) = \frac{\nu}{m^2} \left(c_2^{ab} \log^2 \frac{\nu}{m} + c_1^{ab} \log \frac{\nu}{m} + c_0^{ab} \right) + \frac{\beta_T^{ab}}{m} \left(\frac{\nu}{m} \right)^{\alpha_T(0)} , \quad (2)$$

$$\text{Im } F_{ab}^{(-)}(\nu) = \frac{\beta_V^{ab}}{m} \left(\frac{\nu}{m} \right)^{\alpha_V(0)} , \quad (3)$$

where c_0^{ab} , β_T^{ab} , and β_V^{ab} are unknown parameters in the Pomeron-Reggeon exchange model. The c_2^{ab} and c_1^{ab} are introduced consistently with the Froissart bound to describe the increase of σ_{tot} at high energy. The intercepts are fixed as a common value, with $\alpha_T(0) = \alpha_V(0) = 0.5$. The amplitudes $\text{Im } F_{ab}^{(\pm)}(\nu)$ are related to the total cross sections $\sigma_{\text{tot}}^{\bar{a}\bar{b}, ab}(s)$ by the optical theorem:

$$\begin{aligned} \sigma_{\text{tot}}^{\bar{a}\bar{b}}(s) &= \sigma_{ab}^{(+)}(s) + \sigma_{ab}^{(-)}(s) , \quad \sigma_{\text{tot}}^{ab}(s) = \sigma_{ab}^{(+)}(s) - \sigma_{ab}^{(-)}(s) , \\ \text{where} \quad \sigma_{ab}^{(\pm)}(s) &\equiv \frac{4\pi}{k} \text{Im } F_{ab}^{(\pm)}(\nu) . \end{aligned} \quad (4)$$

In our analysis, $\rho^{\bar{a}\bar{b}, ab}(s)$, the ratios of real to imaginary parts of forward amplitudes, are fitted simultaneously with the data on $\sigma_{\text{tot}}^{\bar{a}\bar{b}, ab}$. Real parts of the crossing-even/odd amplitudes are directly obtained from crossing symmetry $F^{(\pm)}(e^{i\pi}\nu) = \pm F^{(\pm)}(\nu)^*$ as

$$\text{Re } F_{ab}^{(+)}(\nu) = \frac{\pi\nu}{2m^2} \left(c_1^{ab} + 2c_2^{ab} \log \frac{\nu}{m} \right) - \frac{\beta_T^{ab}}{m} \left(\frac{\nu}{m} \right)^{\alpha_T(0)} \cot \frac{\pi\alpha_T(0)}{2} + F_{ab}^{(+)}(0) , \quad (5)$$

$$\text{Re } F_{ab}^{(-)}(\nu) = \frac{\beta_V^{ab}}{m} \left(\frac{\nu}{m} \right)^{\alpha_V(0)} \tan \frac{\pi\alpha_V(0)}{2} . \quad (6)$$

We introduce $F_{ab}^{(+)}(0)$ as a subtraction constant in the dispersion relation [20]. The $\rho^{\bar{a}b,ab}(s)$ are given by

$$\rho^{\bar{a}b,ab}(s) = \text{Re } F^{\bar{a}b,ab}(\nu)/\text{Im } F^{\bar{a}b,ab}(\nu), \quad F^{\bar{a}b,ab}(\nu) = F_{ab}^{(+)}(\nu) \pm F_{ab}^{(-)}(\nu) . \quad (7)$$

2.2 Constrained Analysis with Universal Rise of σ_{tot} and Duality

The contributions of the tensor term in Eq. (2) and the vector term of Eq. (3) to the $\sigma_{\text{tot}}^{\bar{a}b,ab}(s)$ are negligible in the high-energy limit $\sqrt{s} \rightarrow \infty$, where they are well approximated by the $c_{2,1,0}^{ab}$ terms:

$$\sigma_{\text{tot}}^{\bar{a}b}(s) \simeq \sigma_{\text{tot}}^{ab}(s) \simeq B_{ab} \log^2 \frac{s}{s_0^{ab}} + Z_{ab} , \quad (8)$$

$$\text{where} \quad B_{ab} = \frac{4\pi}{m^2} c_2^{ab}, \quad Z_{ab} = \frac{4\pi}{m^2} \left(c_0^{ab} - \frac{c_1^{ab}{}^2}{4c_2^{ab}} \right) , \quad (9)$$

$$s_0^{ab} = 2M\nu_0^{ab} + M^2 + m^2, \quad \nu_0^{ab} = m e^{-\frac{c_1^{ab}}{2c_2^{ab}}} , \quad (10)$$

where s_0^{ab} is a scale for the collision energy squared. By neglecting the small tensor-term contribution, $\sigma_{\text{tot}}^{\bar{a}b,ab}$ develops a minimum Z_{ab} . B_{ab} controls the increase of $\sigma_{\text{tot}}^{\bar{a}b,ab}(s)$ at high energy. In practise, tensor and vector contributions are negligible for $\sqrt{s} \gtrsim 50\text{GeV}$ where $\sigma_{\text{tot}}^{\bar{a}b}$ and σ_{tot}^{ab} are described by Eq. (8).

Two independent analyses [13, 14] of forward $\bar{p}(p)p, \pi^\mp p, K^\mp p$ scattering using finite-energy sum rules (FESR) as constraints, demonstrated that the universality relation

$$B_{pp} = B_{\pi p} = B_{Kp} \equiv B \quad (11)$$

is valid to within one standard deviation. In the present analysis, we will assume this universality from the beginning. It leads to constraints among c_2^{pp} , $c_2^{\pi p}$, and c_2^{Kp} from Eq. (9).

Other powerful constraints are obtained from FESR [5] for crossing-even amplitudes,

$$\frac{2}{\pi} \int_{N_1}^{N_2} \frac{\nu}{k^2} \text{Im} F_{ab}^{(+)}(\nu) d\nu = \frac{1}{2\pi^2} \int_{\overline{N_1}}^{\overline{N_2}} \sigma_{ab}^{(+)}(k) dk = \frac{1}{2\pi^2} \int_{\overline{N_1}}^{\overline{N_2}} (\sigma_{\text{tot}}^{\bar{a}b}(k) + \sigma_{\text{tot}}^{ab}(k))/2 dk , \quad (12)$$

where $\overline{N_{1,2}} = \sqrt{N_{1,2}^2 - m^2}$. The integration limit N_2 is taken in the asymptotically high-energy region, while N_1 is in the resonance-energy region. The left hand side of Eq. (12) is calculated analytically from the asymptotic formula of $\text{Im } F_{ab}^{(+)}$ given by Eq. (2), while the right hand side is estimated from low-energy experimental data. Equation (12) imposes duality on the analysis. It allows us to constrain the high-energy asymptotic behavior with the very precise low energy data, through averaging of the resonances.

Following Ref. [13], we take $\overline{N_1} = 0.818$, 5 , 5 GeV for $ab = \pi p$, pp , Kp , while $\overline{N_2}$ is commonly taken as $\overline{N_2} = 20$ GeV. The FESR (12) yields [13] the constraints,

$$(\pi p) \quad 87.1714\beta_T^{\pi p} + 627.26c_0^{\pi p} + 2572.37c_1^{\pi p} + 10891.2c_2^{\pi p} = 66.961 \pm 0.039, \quad (13)$$

$$(Kp) \quad 8.21363\beta_T^{Kp} + 39.2291c_0^{Kp} + 124.142c_1^{Kp} + 398.549c_2^{Kp} = 38.62 \pm 0.07, \quad (14)$$

$$(pp) \quad 3.14058\beta_T^{pp} + 10.8947c_0^{pp} + 27.5046c_1^{pp} + 71.0017c_2^{pp} = 90.38 \pm 0.20. \quad (15)$$

The integrals of the experimental cross sections in the right hand side are estimated very accurately from low-energy data with errors less than 1%, and these equations can be regarded as exact constraints among parameters.

2.3 Updated Analysis Including LHC and Very High Energy Cosmic-Ray Data

In order to determine the value of B more precisely, we now include three recent measurements, ATLAS, CMS and Auger, covering the very high-energy region in our fit:

- ATLAS reported [21] a pp inelastic cross section $\sigma_{\text{inel}}^{pp}$ at 7 TeV of $69.4 \pm 2.4(\text{exp.}) \pm 6.9(\text{extr.})$ mb where exp./extr. refers to errors from experimental/extrapolation uncertainties. By using the ratio $\sigma_{\text{tot}}/\sigma_{\text{inel}}$ at 7 TeV of 1.38, obtained from the eikonal model [22], σ_{tot}^{pp} is predicted to be $\sigma_{\text{tot}}^{pp}(7 \text{ TeV}) = 96.0 \pm 3.3 \pm 9.5$ mb. Recently, this measurement was confirmed by the CMS collaboration [23] reporting $\sigma_{\text{inel}} = 68.0 \pm 2.0(\text{syst.}) \pm 2.4(\text{lum.}) \pm 4(\text{extr.})$ mb, (where lum. refers to the error associated with the luminosity) giving $\sigma_{\text{tot}}^{pp} = 94.0 \pm 2.8 \pm 3.3 \pm 5.5$ mb at the same energy. We include these data omitting extrapolation errors.
- The Auger [24] collaboration measured $\sigma_{\text{inel}}^{pp}$ at 57 TeV to be $90 \pm 7(\text{stat.})^{+8}_{-11}(\text{syst.}) \pm 1.5(\text{Glauber})$, where the last contribution to the error comes from Glauber theory. Using $\sigma_{\text{tot}}/\sigma_{\text{inel}} = 1.45$ at 57 TeV from Ref. [22], σ_{tot}^{pp} at 57 TeV is predicted to be $131 \pm 10^{+12}_{-16} \pm 2$ mb. We also include this result with statistical error only.

Experimental data of $\sigma_{\text{tot}}^{\bar{a}p,ap}$ at $k \geq 20$ GeV and $\rho^{\bar{a}p,ap}$ at $k \geq 5$ GeV for $\bar{p}(p)p$, $\pi^\mp p$, $K^\mp p$ scattering are fit simultaneously imposing on the parameters $c_{2,1,0}^{ap}$, $\beta_{T,V}^{ap}$, $F_{ap}^{(+)}(0)$ the constraints (11) and (13-15). The highest energy data for $\sigma_{\text{tot}}^{\bar{a}p,ap}$ data reach 26.4(25.3) GeV for $\pi^- p$ ($\pi^+ p$), 24.1 GeV for $K^\mp p$, 1.8 TeV for $\bar{p}p$ (Tevatron), and 57 TeV for pp (Cosmic-Ray).

The number of parameters fitted is $6 \times 3 - 5 = 13$. The fit is very successful despite the omission of systematic errors of the very high-energy data. The total χ^2 is $\chi^2/N_{DF} =$

Table 1: Best-fit parameters of the fit to σ_{tot} and ρ -ratios of $\pi^\mp p$, $K^\mp p$, and $\bar{p}(p)p$ scatterings. Constraints of the universality of B , Eq. (11) and FESR (13-15) are used.

ab	$B(\text{mb})$	$\sqrt{s_0^{ab}}(\text{GeV})$	$Z_{ab}(\text{mb})$	β_T^{ab}	β_V^{ab}	$F_{ab}^{(+)}(0)$
pp	0.280(11)	4.65(42)	35.32(29)	6.71(20)	3.679(36)	10.6(6)
πp	0.280(11)	5.28(32)	21.18(14)	0.155(6)	0.0395(9)	0.12(62)
$K p$	0.280(11)	5.04(30)	17.85(16)	0.446(58)	0.562(8)	2.4(1.0)

431.48/(517 – 13), with χ^2/N_D values of 216.17/244, 150.97/162, and 64.34/111 for $\bar{p}(p)p$, $\pi^\mp p$, and $K^\mp p$ data, respectively. The results of our best fit to $\sigma_{\text{tot}}^{\bar{p}p, pp}$ are shown in Fig. 1. The best-fit values of the parameters are given in Table 1. As shown in Table 1, the universal value of B is obtained by

$$B = 0.280 \pm 0.011 \text{ mb} , \quad (16)$$

which is consistent with our previous estimates,

$$B = 0.2817(64), 0.2792(59) \text{ mb} \quad [4] \quad \text{and} \quad B = 0.280(15) \text{ mb} \quad [13].$$

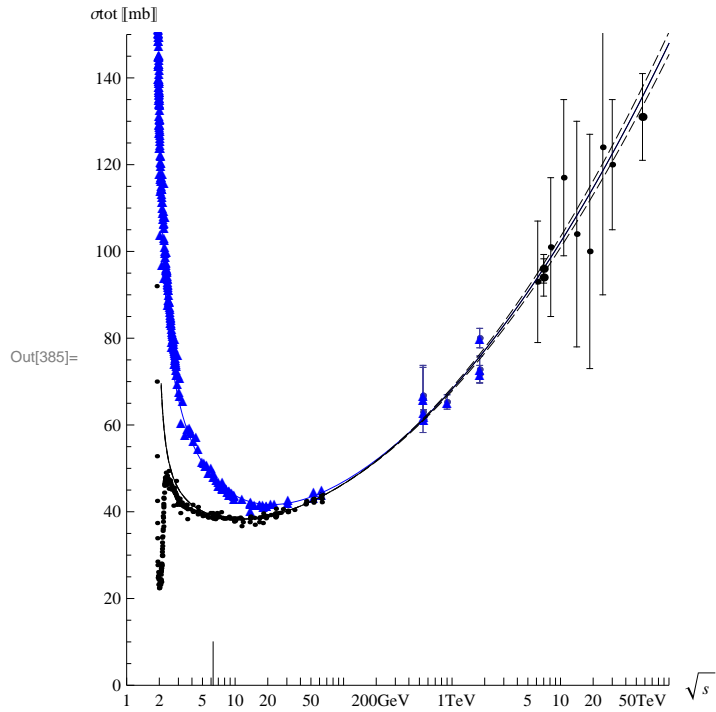


Figure 1: Fit to the data of $\sigma_{\text{tot}}^{\bar{p}p}$ (blue triangles) and σ_{tot}^{pp} (black circles). The solid lines are our best fit and the dashed lines correspond to one standard deviation of B . The vertical line on the x-axis represents the lowest energy of the fit region $\sqrt{s} \geq 6.27$ GeV corresponding to $k \geq 20$ GeV. The LHC ATLAS [21] and CMS [23] data (with no extrapolation errors) at 7 TeV and the Auger data [24] (with only its statistical error) at 57 TeV are shown by bigger black circles.

3 The $\pi\pi$ Total Cross Section

3.1 Theoretical Predictions of $\sigma_{\text{tot}}^{\pi^\mp\pi^+}$

We infer the $\sigma_{\text{tot}}^{\pi^\mp\pi^+}(s)$ based on the analyses of forward $\bar{p}(p)p$, $\pi^\mp p$, and $K^\mp p$ scattering amplitudes. Based on the result of the previous section, we can predict $\sigma_{\text{tot}}^{\pi^\mp\pi^+}$ at high energy. By using the relation $s \simeq 2M\nu$ for $ab = ap = pp, Kp, \pi p$ in high-energies, $\sigma_{\text{tot}}^{\bar{a}p,ap}(s)$ of Eq. (4) can be rewritten in the form

$$\sigma_{\text{tot}}^{\bar{a}p,ap}(s) = B \log^2 \frac{s}{s_0} + Z_{ap} + \tilde{\beta}_T^{ap} \left(\frac{s}{s_1} \right)^{\alpha_T(0)-1} \pm \tilde{\beta}_V^{ap} \left(\frac{s}{s_1} \right)^{\alpha_V(0)-1}, \quad (17)$$

where

$$\tilde{\beta}_{T,V}^{ap} = \frac{4\pi\beta_{T,V}^{ap}}{m^2} \left(\frac{2Mm}{s_1} \right)^{1-\alpha_{T,V}(0)}. \quad (18)$$

s_1 is introduced as a typical scale for the strong interactions which is taken to be $s_1 = 1 \text{ GeV}^2$. It is natural to assume that the universality of B and s_0 extend to $\pi\pi$ scattering. The $\pi^\mp\pi^+$ total cross sections $\sigma_{\text{tot}}^{\pi^\mp\pi^+}$ are expected to take the form

$$\sigma_{\text{tot}}^{\pi^\mp\pi^+}(s) = B \log^2 \frac{s}{s_0} + Z_{\pi\pi} + \tilde{\beta}_T^{\pi\pi} \left(\frac{s}{s_1} \right)^{\alpha_T(0)-1} \pm \tilde{\beta}_V^{\pi\pi} \left(\frac{s}{s_1} \right)^{\alpha_V(0)-1}, \quad (19)$$

where B and s_0 are given by Eq. (17).

The values of $Z_{\pi p}, Z_{Kp}, Z_{pp}$ in Table 1 approximately satisfy the ratios predicted by the quark model.

$$Z_{\pi p} : Z_{Kp} : Z_{pp} = 21.18 : 17.85 : 35.32 \simeq 2 : 2 : 3. \quad (20)$$

By using the quark model meson/baryon ratio, $Z_{\pi\pi}$ is $Z_{\pi\pi} = \frac{2}{3}Z_{\pi p} = 14.1 \text{ mb}$, while the $Z_{\pi\pi}$ is also given by $Z_{\pi\pi} = \frac{Z_{\pi p}}{Z_{pp}}Z_{\pi p} = 12.7 \text{ mb}$, where the meson/baryon ratio is taken to be $Z_{\pi p}/Z_{pp} = 0.60$ instead of $2/3$. This assumes that the Z_{ab} terms represent the conventional Pomeron exchange with a unit intercept (and no logarithmic terms) and that its coupling satisfies the Regge factorization. So our prediction is

$$Z_{\pi\pi} = (12.7 \pm 1.4) \text{ mb}, \quad (21)$$

where the error is estimated from the difference between the above estimates. Actually this is the main source of uncertainty for our prediction at very high energy. Presently we have no rigorous theoretical way to estimate the accurate value of $s_0^{\pi\pi}$, hence, we assume for simplicity

$$\sqrt{s_0^{\pi\pi}} \approx \sqrt{s_0^{\pi p}} = 5.28 \pm 0.63 \text{ GeV}, \quad (22)$$

where the error comes from a difference between $s_0^{\pi p}$ and s_0^{pp} for our best fit given in Table 1.

The coefficients $\tilde{\beta}_{T,V}^{ab}$ take multiplicative forms in terms of Reggeon- $aa(bb)$ couplings $\gamma_{Raa,Rbb}$ with $\tilde{\beta}_T^{ab} = \gamma_{Taa} \gamma_{Tbb}$ and $\tilde{\beta}_V^{ab} = \gamma_{Vaa} \gamma_{Vbb}$. In the case $ab = pp$ and Kp , both $f_2(1270)$ and $a_2(1320)$ -trajectories contribute via the tensor-meson term and both ρ and ω -trajectories contribute through the vector-meson term, while in the case $ab = \pi p$ and $\pi\pi$ only the former trajectories contribute through the tensor and vector terms. Using Eq. (18), the values of $\tilde{\beta}_{T,V}^{ap}$ are obtained from Table 1:

$$\begin{aligned} \tilde{\beta}_T^{\pi p} &= \frac{\gamma_{f_2\pi\pi}\gamma_{f_2pp}}{= 19.9 \text{ mb}}, & \tilde{\beta}_V^{\pi p} &= \frac{\gamma_{\rho\pi\pi}\gamma_{\rho pp}}{= 5.07 \text{ mb}}, \\ \tilde{\beta}_T^{Kp} &= \frac{\sum_{R=f_2,a_2}\gamma_{RKK}\gamma_{Rpp}}{= 8.62 \text{ mb}}, & \tilde{\beta}_V^{Kp} &= \frac{\sum_{R=\rho,\omega}\gamma_{RKK}\gamma_{Rpp}}{= 10.9 \text{ mb}}, \\ \tilde{\beta}_T^{pp} &= \frac{\gamma_{f_2pp}^2 + \gamma_{a_2pp}^2}{= 49.5 \text{ mb}}, & \tilde{\beta}_V^{pp} &= \frac{\gamma_{\rho pp}^2 + \gamma_{\omega pp}^2}{= 27.1 \text{ mb}}. \end{aligned} \quad (23)$$

The γ -couplings are expected to approximately satisfy SU(2) and SU(3) flavor symmetry: $\gamma_{f_2pp} = \gamma_{a_2pp}$, $\gamma_{\rho pp} = \gamma_{\omega pp}$ and $\gamma_{\rho\pi\pi}/2 = \gamma_{\rho KK} = \gamma_{\omega KK}$, $\gamma_{f_2\pi\pi}/2 = \gamma_{f_2KK} = \gamma_{a_2KK}$. From SU(3), $\tilde{\beta}_{T,V}^{\pi p} = \tilde{\beta}_{T,V}^{Kp}$ is expected, although it is violated; see Eq. (23). On the other hand, for $\pi\pi$ scattering, $\tilde{\beta}_T^{\pi\pi} = \gamma_{f_2\pi\pi}^2$ and $\tilde{\beta}_V^{\pi\pi} = \gamma_{\rho\pi\pi}^2$. They can be evaluated from the results of $\bar{p}(p)p$ and $\pi^\mp p$ of Eq. (23) using SU(2) relations only:

$$\tilde{\beta}_T^{\pi\pi} = \frac{(19.9)^2}{49.5/2} \text{ mb} = 16.0 \pm 3.9 \text{ mb}, \quad \tilde{\beta}_V^{\pi\pi} = \frac{(5.07)^2}{27.1/2} \text{ mb} = 1.9^{+1.9}_{-1.0} \text{ mb}, \quad (24)$$

where the error of $\tilde{\beta}_T^{\pi\pi}$ is taken from its difference from $\tilde{\beta}_T^{\pi p}$. By considering $\tilde{\beta}_V^{\pi p}/\tilde{\beta}_V^{Kp} \simeq 1/2$, our prediction of $\tilde{\beta}_V^{\pi\pi}$ may possibly include factor $\sim 1/2$ uncertainty which motivates the error in Eq. (24).

Table 2: Numerical values for the predictions of $\sigma_{\text{tot}}^{\pi^\mp\pi^\pm}$ and their difference for a range of energies. Uncertainties from the errors of $\tilde{\beta}_{T,V}^{\pi\pi}$ decrease with the increasing energies, and become negligible above $\sqrt{s} \sim 40 \text{ GeV}$, while the uncertainties from the errors on $B (= 0.280 \pm 0.011 \text{ mb})$ and $\sqrt{s_0} (= 5.28 \pm 0.63 \text{ GeV})$ become sizable above this energy.

$\sqrt{s}(\text{GeV})$	$\sigma_{\text{tot}}^{\pi^-\pi^+}(\text{mb})$	$\sigma_{\text{tot}}^{\pi^+\pi^+}(\text{mb})$	difference(mb)
3	$19.0 \pm 1.4_Z \pm 1.3_{\tilde{\beta}_T}$	$17.7 \pm 1.4_Z \pm 1.3_{\tilde{\beta}_T}$	$1.3^{+1.4}_{-0.7} \tilde{\beta}_V$
5	$16.3 \pm 1.4_Z \pm 0.8_{\tilde{\beta}_T}$	$15.5 \pm 1.4_Z \pm 0.8_{\tilde{\beta}_T}$	$0.8^{+0.8}_{-0.4} \tilde{\beta}_V$
10	$15.0 \pm 1.4_Z \pm 0.4_{\tilde{\beta}_T}$	$14.6 \pm 1.4_Z \pm 0.4_{\tilde{\beta}_T}$	$0.4^{+0.4}_{-0.2} \tilde{\beta}_V$
20	$15.6 \pm 1.4_Z \pm 0.3_{s_0} \pm 0.2_{\tilde{\beta}_T}$	$15.4 \pm 1.4_Z \pm 0.3_{s_0} \pm 0.2_{\tilde{\beta}_T}$	$0.2^{+0.2}_{-0.1} \tilde{\beta}_V$
40	$17.74 \pm 1.4_Z \pm 0.5_{s_0} \pm 0.2_B$	$17.64 \pm 1.4_Z \pm 0.5_{s_0} \pm 0.2_B$	$0.1^{+0.1}_{-0.05} \tilde{\beta}_V$
50	$18.7 \pm 1.4_Z \pm 0.6_{s_0} \pm 0.2_B$		0.08
100	$22.5 \pm 1.4_Z \pm 0.7_{s_0} \pm 0.4_B$		0.0
200	$27.6 \pm 1.4_Z \pm 0.9_{s_0} \pm 0.6_B$		0.0
500	$35.9 \pm 1.4_Z \pm 1.1_{s_0} \pm 0.9_B$		0.0
1000	$43.5 \pm 1.4_Z \pm 1.3_{s_0} \pm 1.2_B$		0.0

In summary, $\sigma_{\text{tot}}^{\pi^\mp\pi^+}(s)$ are predicted by Eq. (19) with the parameters B from Eq. (16), $Z_{\pi\pi}$ from Eq. (21), $s_0^{\pi\pi}$ from Eq. (22), and $\tilde{\beta}_{T,V}^{\pi\pi}$ from Eq. (24). The numerical values of our predictions for several \sqrt{s} -values are given in Table 2.

3.2 Comparison with Indirect Experiments

There are no direct measurements of $\sigma_{\text{tot}}^{\pi\pi}$ at present, however, indirect data at low- and intermediate-energy have been extracted [18, 19, 25, 26] from processes with $\pi\pi$ final states. They are shown in Fig. 2.

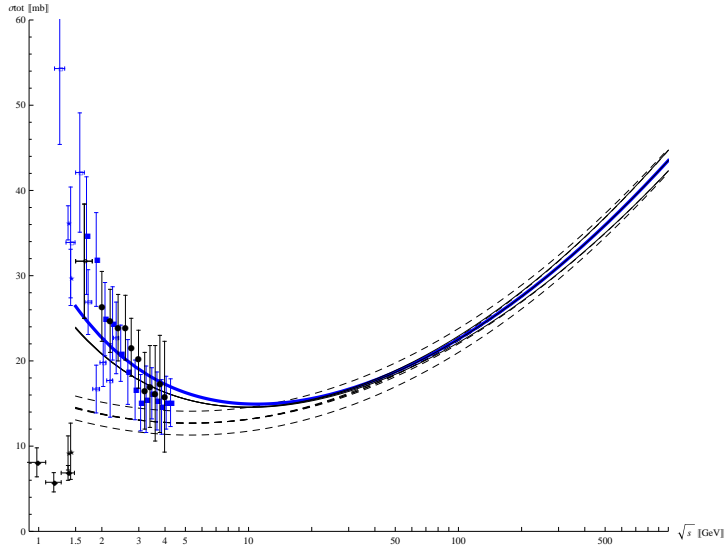


Figure 2: $\pi^\mp\pi^+$ total cross section (mb) versus \sqrt{s} . $\sigma_{\text{tot}}^{\pi^-\pi^+}$ (thick solid blue) and $\sigma_{\text{tot}}^{\pi^+\pi^+}$ (thin solid black). The dashed lines only show the contribution from $B \log^2 s / s_0 + Z_{\pi\pi}$, and their difference is the error on $Z_{\pi\pi}$. Uncertainties from the errors of B , which are shown by black solid lines, are not dominant for \sqrt{s} less than 1 TeV. The uncertainty from the errors of $\sqrt{s_0}$ are not shown in this figure; they have the same tendency as those from B . Dot-dashed lines represent the error from the uncertainty of $\tilde{\beta}_T^{\pi\pi}$. The f_2 and ρ trajectories have sizable contributions below $\sqrt{s} = 30$ GeV. Our predictions are expected to be applicable for $\sqrt{s} \gtrsim 3$ GeV, although their low-energy extensions are also shown. The $\pi^-\pi^+$ data are blue and large solid /small open squares, while the $\pi^-\pi^-$ data are black and large solid/small open circles (Here we assume $\sigma_{\text{tot}}^{\pi^-\pi^-} = \sigma_{\text{tot}}^{\pi^+\pi^+}$ from CPT invariance); they are from Robertson73 [18]/Biswas67 [19]. For data below 1.5GeV, the stars are from Pelaez03 [26, 27] and the solid diamonds are from Cohen73 [25]. We removed the lowest-energy (1.35GeV) datum of $\sigma_{\text{tot}}^{\pi^-\pi^-}$ of Ref. [19], since at this energy the elastic amplitude $f(s, 0)$ is approximately real (which is consistent with the result of Cohen73 [25] that S -wave phase shift is small, about -30° , and $\sigma_{\text{inel}}^{\pi^-\pi^-} / \sigma_{\text{el}}^{\pi^-\pi^-} \sim 0.2$), and the basic assumption that $f(s, 0)$ is imaginary is not satisfied.

The data have large errors, however, our predictions coincide with the data [18] starting at moderate energies. The $\pi^\pm\pi^-$ data in $3 \leq \sqrt{s} \leq 4.25$ GeV are 13 points, which give a good χ^2 for our prediction although there are no fitting parameters: $\chi^2/N_{DF} = 5.08/13$; for $\pi^+\pi^-(\pi^-\pi^-)$,

$$\chi^2/N_D = 4.50/7 \text{ (0.58/6).}$$

The experimental data for $\sigma_{\text{tot}}^{\pi^-\pi^-}$ have a tendency to give larger values than those for $\sigma_{\text{tot}}^{\pi^-\pi^+}$, notwithstanding that Regge theory requires the opposite. This seems to be due to a systematic uncertainty of the experiments since $\sigma_{\text{tot}}^{\pi^-\pi^+}$ and $\sigma_{\text{tot}}^{\pi^-\pi^-}$ are extracted from different processes, $\pi^-p \rightarrow \pi^-\pi^+n$ and $\pi^-p \rightarrow \pi^-\pi^-\Delta^{++}(1232)$, respectively. Anyway, a very small difference between $\sigma_{\text{tot}}^{\pi^-\pi^+}$ and $\sigma_{\text{tot}}^{\pi^-\pi^-}$ seems to be suggested in the intermediate-energy region $\sqrt{s} \sim 3 \text{ GeV}$. This is consistent with our prediction of very small $\tilde{\beta}_V^{\pi\pi}$ in Eq. (24).

Values for $\sigma_{\text{tot}}^{\pi\pi}$ have been extracted from other indirect processes without detecting $\pi\pi$ in final states, such as $\pi^\pm p \rightarrow X\Delta^{++}$, $\pi^\pm n \rightarrow Xp$ [28, 29, 30], using the Reggeized pion method applied to $|t|$ -regions far from the pion pole. This method includes inevitably large theoretical uncertainties from the exchanges of various mesons, $\rho, a_1(1260), a_2(1320), \dots$ and their corresponding trajectories. We have omitted these data from our analysis.

The authors in Ref. [26] analyze $\sigma_{\text{tot}}^{\pi^\mp p}$, $\sigma_{\text{tot,pp}}^{(+)} (= (\sigma_{\text{tot}}^{\bar{p}p} + \sigma_{\text{tot}}^{pp})/2)$ and $\pi^\pm\pi^-$ data simultaneously. All the data, including [29, 30], as well as the data with very low energies, $\sqrt{s} = 1.38, 1.42 \text{ GeV}$ [26, 27], are included in their fit. Their value for $\beta_\rho/\beta_{P'} = 1.0/1.05$ is much larger than our prediction $\tilde{\beta}_V^{\pi\pi}/\tilde{\beta}_T^{\pi\pi} = (1.9^{+1.9}_{-1})/16$. However, at energies of $\sqrt{s} = 1.38, 1.42 \text{ GeV}$, only a limited number of inelastic channels are present and Regge theory should not apply. Above these energies $\sigma_{\text{tot}}^{\pi^-\pi^-}$ is expected to show a rapid growth, similar to the experimental data for σ_{tot} of the other exotic channels, K^+p and pp .

4 Discussion and Conclusion

Our predictions for $\sigma_{\text{tot}}^{\pi^\mp\pi^+}$ are shown along with the results of our best fit for $\sigma_{\text{tot}}^{\pi^\mp p}$ and $\sigma_{\text{tot}}^{\bar{p}(p)p}$ in Fig. 3. The difference in normalization of these curves is determined by the Z_{ab} , $Z_{pp} > Z_{\pi p} > Z_{\pi\pi}$, while their increase with energy is described by the universal value of B , Eq. (16).

There are a few comments as our concluding remarks:

- We have previously predicted the σ_{tot}^{pp} for LHC and cosmic-ray energies in [4, 13]. Now our previous predictions can be tested by using the new experimental data [21, 23, 24] shown in Table 3. The result of the fit in the present work is also shown, together with the predictions at $\sqrt{s} = 14 \text{ TeV}$. As can be seen in this table, our predictions are in excellent agreement with the experiments. The best-fit value of B in the present analysis that includes these new data completely coincides with our previous values, see Eq. (16). This remarkable agreement is achieved, in our opinion, by including the information from low-energy data using the duality constraints.

Table 3: Comparison of our previous predictions of σ_{tot}^{pp} (mb) with the new experiments by ATLAS [21], CMS [23], and Auger [24]. The result of the fit in the present work is also given. For the derivation of the experimental values, see the text. The numbers with parentheses are the fit results, and the others are predictions.

\sqrt{s} (TeV)	σ_{tot}^{pp} (BH)[4]	σ_{tot}^{pp} (II)[13]	this work	σ_{tot}^{pp} (mb) (exp.)
7	95.4 ± 1.1	96.0 ± 1.4	(96.1 ± 1.1)	$96.0 \pm 3.3_{\text{exp.}} \pm 9.5_{\text{extr.}}$: ATLAS $94.0 \pm 2.8_{\text{Syst.}} \pm 3.3_{\text{Lum.}} \pm 5.5_{\text{Extr.}}$: CMS
14	107.3 ± 1.2	108.0 ± 1.9	108.1 ± 1.4	
57	134.8 ± 1.5	135.5 ± 3.1	(135.7 ± 2.2)	$131 \pm 10_{\text{Stat.}} \pm 16_{\text{Syst.}} \pm 2_{\text{Glauber}}$: Auger

- The COMPETE collaboration assumed the universality of s_0 in their fit [3, 7]. By adopting this s_0 -universality and applying the further constraints $s_0^{pp} = s_0^{\pi p} = s_0^{Kp}$ in our analysis, we obtain $B = 0.299(8)$ mb and the universal $\sqrt{s_0} = 5.59(30)$ GeV, which are consistent with $B = 0.308(10)$ mb and $\sqrt{s_0} = 5.38(50)$ GeV of COMPETE collaboration [3, 7]. However, because of a strong correlation between B and $\sqrt{s_0^{ap}}$, the above B -value is slightly larger than our best fit Eq. (16) and the universal $\sqrt{s_0} = 5.59$ GeV is slightly larger than the values of $\sqrt{s_0^{pp}}$, $\sqrt{s_0^{Kp}}$, and $\sqrt{s_0^{\pi p}}$ in Table 1. The resulting χ^2 of the analysis with the $\sqrt{s_0}$ universality is $\chi^2/N_{DF} = 438.53/(517-11)$, which becomes worse by a factor 7 (for extra 2 constraints) compared with our best fit $\chi^2/N_{DF} = 431.48/(517-13)$. The s_0 -universality is disfavored. So we did not adopt it in the present analyses for $\bar{p}(p)p$, $\pi^\mp p$, $K^\mp p$ scatterings.
- We predict a very small value of $\tilde{\beta}_V^{\pi\pi}$ in the Reggeon-exchange model in Eq. (24). This value seems to be natural since the experimental data in Fig. 3 clearly suggest $\sigma_{\text{tot}}^{\pi^- p} - \sigma_{\text{tot}}^{\pi^+ p} \ll \sigma_{\text{tot}}^{\bar{p} p} - \sigma_{\text{tot}}^{p p}$ in the intermediate region. The authors of Ref. [31] predict a large value of $\tilde{\beta}_V^{\pi\pi}$ that is inconsistently with ours, although the method is the same. The authors [26] discussed the consistency check by using the second sum rule for the crossing-odd amplitude, which corresponds to the $n = -2$ moment sum rule. They apply this sum rule to the Regge formula with only a single term for the ρ -trajectory and obtained a large value of $\beta_\rho = 0.82 \pm 0.12$. They considered a smooth extrapolation from the low-energy $\pi\pi$ amplitude below 1.8 GeV, similar to Ref. [32]. However, this sum rule emphasizes strongly the contributions from very low energies, and we are forced to consider the contribution of the ρ' trajectory, the daughter of ρ -trajectory. Since we have no estimate of its intercept, a sum rule of this type cannot constrain the value of β_ρ .

Note added in proof – After completing the manuscript, we found that the TOTEM [33] has

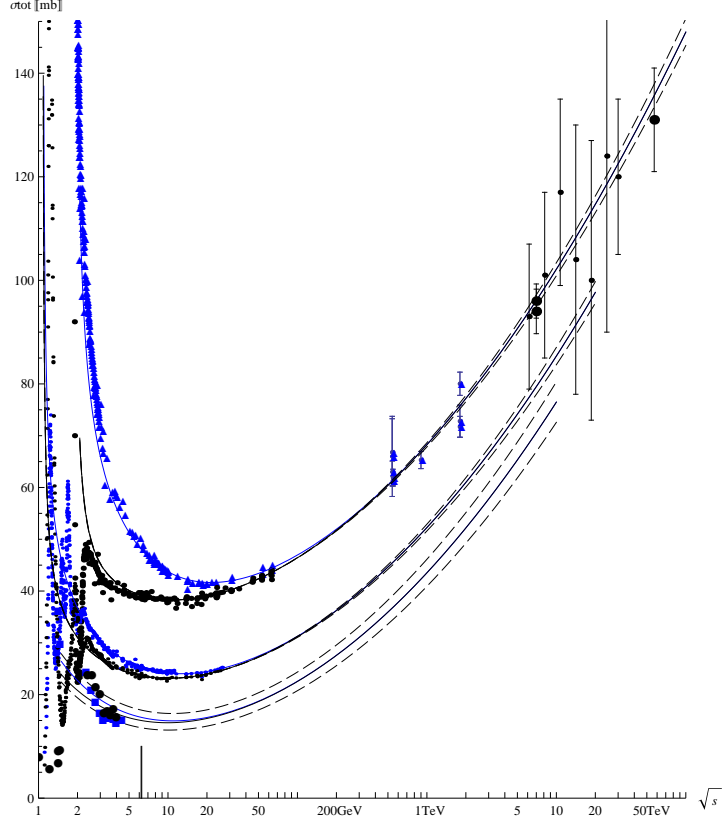


Figure 3: Total cross sections(mb) versus \sqrt{s} . Solid lines are $\bar{p}p, pp, \pi^- p, \pi^+ p, \pi^- \pi^+, \pi^+ \pi^+$ from up-to-down. $\bar{p}p, pp$ and $\pi^- p, \pi^+ p$ are our best fit, while $\pi^- \pi^+, \pi^+ \pi^+$ are our predictions. The dot-dashed lines represent the upper(lower)-limit of our predictions of $\sigma_{\text{tot}}^{\pi^- \pi^+} (\sigma_{\text{tot}}^{\pi^+ \pi^+})$. Dashed lines for $\bar{p}(p)p$ and $\pi^\mp p$ represent the uncertainties of our predictions which are obtained from the errors of B and $Z_{\pi\pi}$. For $\sigma_{\text{tot}}^{\pi^+ \pi^-} / \sigma_{\text{tot}}^{\pi^- \pi^-}$ data are shown by solid squares/circles, the data [18] in $\sqrt{s} \geq 2.2$ GeV, the data [26, 27] at $\sqrt{s} = 1.38, 1.42$ GeV, and the $\sigma_{\text{tot}}^{\pi^- \pi^-}$ data [25] are shown.

measured a total proton-proton cross section at $\sqrt{s} = 7$ TeV, $98.3 \pm 0.2(\text{stat.}) \pm 2.8(\text{syst.})$ mb, which is a somewhat large value but consistent with our prediction 96.1 ± 1.1 mb within the errors.

Acknowledgments

F.H. is supported by the National Science Foundation award 096906. M.I. is very grateful to Dr. R. Kaminski for informing me the $\pi\pi$ data and giving crucial comments. This work is supported in part by KAKENHI (2274015, Grant-in-Aid for Young Scientists(B)) and in part by grant as Special Researcher of Meisei University. C.S.K. is supported by Basic Science Research Program through the NRF of Korea funded by MOEST (No. 2011-0027275), (No. 2011-0017430) and (No. 2011-0020333).

References

- [1] M. M. Block, F. Halzen, [arXiv:1109.2041 [hep-ph]].
- [2] K. Igi, M. Ishida, Phys. Rev. D **66**, 034023 (2002).
- [3] J.R.Cudell et al. (COMPETE Collab.), Phys. Rev. D **65**, 074024 (2002).
- [4] M. M. Block, F. Halzen, Phys.Rev. D **72**,036006 (2005).
- [5] K. Igi, M. Ishida, Phys. Lett. B **622** (2005) 286.
- [6] M. Froissart, Phys. Rev. **123**, 1053 (1961).
A. Martin, Nuovo Cimento **42**, 930 (1966).
- [7] K. Nakamura et al. (Particle Data Group), J. Phys. G **37**, 075021 (2010).
- [8] L. L. Jenkovszky, B. V. Struminsky and A. N. Wall, Yad. Fiz. **46**, 1519 (1987). ‘Where is “asymptopia”?’, 1986, ITP-86-82E.
- [9] J. Finkelstein, H. M. Fried, K. Kang, and C.-I. Tang, Phys. Lett. B **232**, 257 (1989).
- [10] E. Ferreiro, E. Iancu, K. Itakura, L. McLerran, Nucl. Phys. A **710**, 373 (2002).
- [11] L. Frankfurt, M. Strikman, M. Zhalov, Phys. Lett. B **616**, 59 (2005).
- [12] M. M. Block, E. M. Gregores, F. Halzen and G. Pancheri, arXiv: hep-ph/9809403v1.
- [13] M. Ishida, K. Igi, Phys. Rev. D **79**, 096003 (2009).
M. Ishida, K. Igi, Phys. Lett. B **670**, 397 (2009).
- [14] M. Ishida and V. Barger, Phys. Rev. D **65**, 116005 (2001).
- [15] “A white paper based on the Project X Physics Workshop”, November 2009.
- [16] Japan Proton Accelerator Research Complex, <http://j-parc.jp/index-e.html>.
- [17] Private communication with S. Geer.
- [18] W. J. Robertson, W. D. Walker and J. L. Davis, Phys. Rev. D **7**, 2554 (1973).
- [19] N. N. Biswas, N. M. Cason, I. Derado, V. P. Kenney, J. A. Poirier, and W. D. Shephard, Phys. Rev. Lett. **18**, 273 (1967).

- [20] M. M. Block, Phys. Rev. D **65**, 116005 (2002).
- [21] The ATLAS Collaboration, arXiv:1104.0326v1 [hep-ex].
- [22] M. M. Block and F. Halzen, arXiv:1102.3163.
- [23] The CMS Collaboration, “Measurement of the inelastic pp cross section at $\sqrt{s} = 7$ TeV with the CMS detector”, CMS Physics Summary 2011/08/10.
- [24] The Auger Collaboration, arXiv:1107.4804 [astro-physics.HE], (2011), part 2., “Estimate of the proton-air cross section”, R. Ulrich; Auger Collaboration, M. Mostafa, XXXI Physics in Collision Conference, Vancouver, Sept 1 2011.
- [25] D. Cohen, T. Ferbel, P. Slattery, and B. Werner, Phys. Rev. D **7**, 661 (1973).
- [26] J. R. Pelaez and F. J. Yndurain, Phys. Rev. D **69**, 114001 (2004).
- [27] J. R. Pelaez and F. J. Yndurain, Phys. Rev. D **68**, 074005 (2003).
- [28] B. G. Zakharov and V. N. Sergeev, Yad. Fiz. **39**, 707 (1984) [Sov. J. Nucl. Phys. **39**, 448 (1984)].
- [29] J. Hanlon, A. Brody, E. Engelman, T. Kafka, H. Wahl, A. A. Seidl, W. S. Toothacher, J. C. Vander Velde, M. Binkley, J. E. A. Lys, C. T. Murphy, S. Dado, A. Engler, G. Keyes, R. W. Kraemar, and G. Yekutieli, Phys. Rev. Lett. **37**, 967 (1976).
- [30] H. Abramowicz, M. Gorski, G. Sinapius, A. Wroblewski, A. Ziemiński, H. J. Lubatti, K. Moriyasu, C. D. Rees, D. Kisielewska, J. Figiel, L. Suszycki, K. Sliwa, W. Ko, J. S. Pearson and P. Yager, Nucl. Phys. B **166**, 62 (1980).
- [31] A. Szczurek, N. N. Nikolaev, and J. Speth, hep-ph/0112331v1.
- [32] C. D. Froggatt and J. L. Petersen, Nucl. Phys. B **129**, 89 (1977).
- [33] The TOTEM Collaboration, “First measurement of the total proton-proton cross section at the LHC energy of $\sqrt{s} = 7$ TeV”, CERN-PH-EP-2011-158.